sustainability

MDPI

Article

Long-Term Correlations and Cross-Correlations in Meteorological Variables and Air Pollution in a Coastal Urban Region

Anderson Palmeira [1], Éder Pereira [2], Paulo Ferreira [3,4,5,*], Luisa Maria Diele-Viegas [6] and Davidson Martins Moreira [1]

1 Manufacturing and Technology Integrated Campus, SENAI CIMATEC, Salvador 41650-010, Bahia, Brazil
2 Instituto Federal do Maranhão, Bacabal 65700-000, Maranhão, Brazil
3 VALORIZA—Research Center for Endogenous Resource Valorization, 7300-555 Portalegre, Portugal
4 Department of Economic Sciences and Organizations, Polytechnic Institute of Portalegre, 7300-555 Portalegre, Portugal
5 CEFAGE, IIFA, Universidade de Évora, Largo dos Colegiais 2, 7004-516 Évora, Portugal
6 Instituto de Biologia, Universidade Federal da Bahia, Salvador 40170-115, Bahia, Brazil
* Correspondence: pferreira@ipportalegre.pt

Abstract: In this work, we evaluated the evolution of some atmospheric pollutants (O_3, NOx and PM10) over time and their relationship with four different climate variables (solar irradiation, air temperature, relative humidity and wind speed). To this end, we assessed the long-range dependence of those concentrations with a Detrended Fluctuation Analysis (DFA) and analyzed the cross-correlation of such dependence with the climate variables through a Detrended Cross-Correlation Coefficient Analysis ($\rho DCCA$). The results show that air pollution tends to increase over time, impairing air quality and likely affecting human health. The results indicate a cross-correlation between air pollution and the climatic variables, which persisted for a certain period, with a greater correlation between O_3 concentration and wind, mainly temperature, and a negative correlation with humidity for all monitoring stations. Moreover, unlike O_3 and PM10, NOx concentrations always had a persistent behavior in the region of study for the entire analyzed period.

Keywords: air pollution; detrended cross-correlation analysis; emissions; long memory

Citation: Palmeira, A.; Pereira, É.; Ferreira, P.; Diele-Viegas, L.M.; Moreira, D.M. Long-Term Correlations and Cross-Correlations in Meteorological Variables and Air Pollution in a Coastal Urban Region. *Sustainability* **2022**, *14*, 14470. https://doi.org/10.3390/su142114470

Academic Editors: Pallav Purohit and Sudhir Kumar Pandey

Received: 14 September 2022
Accepted: 1 November 2022
Published: 4 November 2022

1. Introduction

Atmospheric pollution is a critical factor impairing biodiversity, ecosystem services and human health [1]. The increase in pollutant concentrations due to the growth of urban and industrial areas has led to the rise in scientific discussions on this topic [2–10]. The concentration level of atmospheric pollutants (gases and particles) is correlated with the combination of meteorological variables in a given region. Therefore, the concentration of atmospheric pollutants and the meteorological data must be statistically evaluated to verify their correlations, being an important topic in atmospheric dispersion problems. In this sense, natural phenomena dynamics are characterized by long-range correlations, where the autocorrelation function varies according to a potency law [11,12]. Thus, the applicability of mathematical modeling in the description and interpretation of these dynamics constitutes a valuable tool for solving real problems and for reasoning decisions [13]. Specifically, determining a long-range correlation between pollutant emissions (pollutant concentrations are the consequences of emissions) and environmental changes demands understanding non-stationary processes such as global circulation patterns and global warming tendencies [14].

The DFA (Detrended Fluctuation Analysis) method was developed to extract long-range correlation in non-stationary temporal series [15], becoming an important tool for understanding such complex processes. It was applied in studies focusing on several

topics, including environmental temperature behavior [16], wind speed [17–20], precipitation [21], relative humidity [22] and the North Atlantic Oscillation Index [23]. On the other hand, the $\rho DCCA$ (Detrended Cross-Correlation Coefficient Analysis) statistical model, was developed to evaluate cross-correlations among pairs of non-stationary temporal series [24]. If compared, for example, with Pearson's coefficient, it is robust [25]. Some works, such as [26], applied the $\rho DCCA$ to highly complex empirical data from financial markets. In [27–29], it is analyzed how external meteorological variables are related, as is proposed in this work with the $\rho DCCA$ multiple cross-correlation coefficients. In [30], cross-correlations between three meteorological variables at the same time are analyzed; in [31], $\rho DCCA$ is applied to identify and characterize correlated data obtained from drilled oil wells; in [32], the $\rho DCCA$ cross-correlation coefficient method is adopted to quantify cross-correlations between energy markets and emissions. Ref. [33] established a well-defined relationship between αDFA (the long-range auto-correlation exponent) and $\lambda DCCA$ (the long-range cross-correlation exponent), described by the DFA and DCCA methods, respectively. Ref. [34] theoretically studied several fundamental properties of the DCCA cross-correlation coefficient, which contributes to acquire more statistical characteristics of this measure. Ref. [35] investigated power law cross-correlations between different time series recorded simultaneously in the presence of non-stationarity. Ref. [36] analyzed and quantified cross-correlation between climatological data, adopting the DCCA and $\rho DCCA$ cross-correlation coefficients. In [37], the cross-correlation between air temperature and relative humidity is studied using the DCCA cross-correlation coefficient. Furthermore, [27] proposed to establish an extended multiple cross-correlation coefficient, and [30] analyzed the cross-correlations in non-stationary time series.

Various studies show that the analysis of data over time allows guiding control actions. In this way, persistence is evaluated, since persistent series tend to increase over time, so that if the concentrations of pollutants show an increasing trend, the risks of air quality will increase, which may, therefore, affect health human. In this sense, the literature is still incipient to correlate the concentration of atmospheric pollutants and meteorological variables, as proposed in this work. Understanding air pollution patterns and tendencies is paramount to predicting, evaluating and mitigating its impacts on social, economic and environmental systems.

Our objective is to show whether there are strong correlations between meteorological factors and pollutants' concentration in the port area of Aratu, Brazil, as well as to statistically evaluate the persistence. The proposed methodologies to analyze persistence and correlation can be used to test the suitability of complex numerical meteorological and air pollution models, with the possibility to predict the results of pollution, since these models must reproduce the effects of long-term memory, which may represent an important advancement in the research area of atmospheric sciences. In particular, we aimed to assess the long-term evolution and persistence of the air pollutant dispersion data from industrial activities in the influence area of the port of Aratu, one of the most important outlets for chemical and petrochemical production, located in Bahia State, Brazil, by using DFA analysis. In addition, we aimed to evaluate the influence of climatic variables (e.g., environmental temperature, relative air humidity, wind velocity and solar radiation) on the pollution process through $\rho DCCA$ analysis.

This paper is organized as follows. Section 2 presents the materials and methods, including the study area, experimental data and a brief review of DFA and $\rho DCCA$ methodologies. Section 3 presents the numerical results, applying DFA and $\rho DCCA$ to investigate the long-range and cross-correlations between the concentrations of pollutants and each meteorological factor. Section 4 draws the conclusions.

2. Materials and Methods

2.1. Study Area

The study area is the Metropolitan Region of Salvador (RMS), located in the state of Bahia, between latitudes 12°20′ S and 13°10′ S and longitudes 37°50′ W and 38°50′ W,

comprising 13 cities. It is occupied by approximately 3.6 million inhabitants spread over an area of 4.375 km^2. The RMS is an urban-industrial area with a peninsular configuration and consists of a bay located in the southwest of the region, east of the Atlantic Ocean. The Baía de Todos os Santos (BTS) is an indentation of the Brazilian coast where the sea penetrates the continent from a narrowing between the city of Salvador, which is the capital of the state of Bahia, and the island of Itaparica. Its presence adds local moisture due to evaporation, forming a humid tropical climate in the region. The period with the highest rainfall is April–May–June–July, while the least rainy period is September–October–November–December. The annual averages of temperature and humidity are 26 °C and 80%, respectively, in Salvador, with higher values of average hourly wind speed in the afternoon and lower values during dawn and early morning hours [38]. Figure 1 shows the studied location.

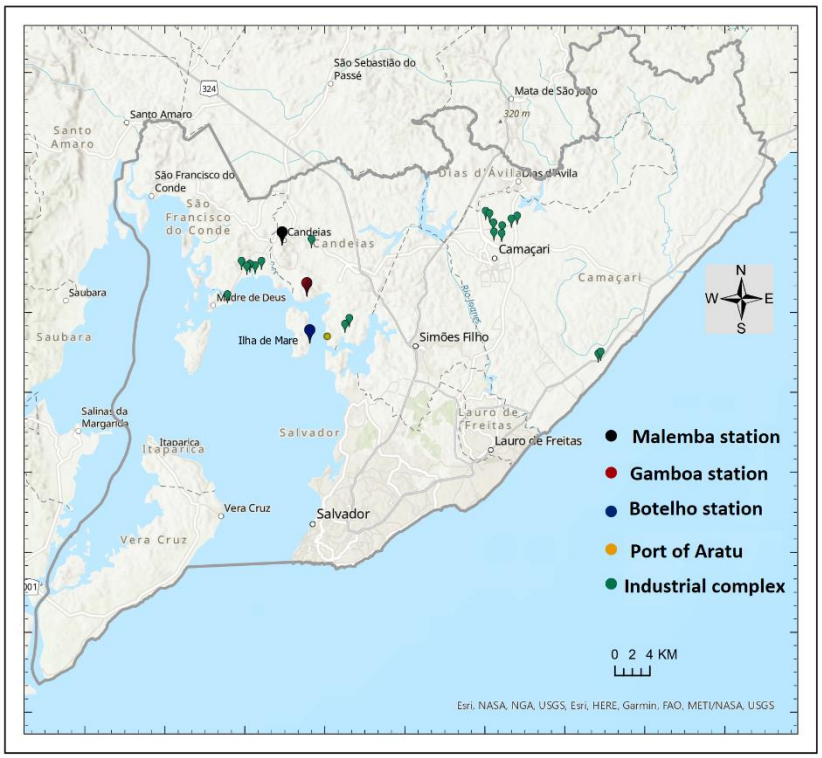

Figure 1. The three air monitoring stations located in Botelho, Malembá and Gamboa regions located in Todos os Santos Bay, Bahia, Brazil.

Figure 1 shows the three air quality stations (Malembá, Gamboa and Botelho) and some fixed sources (industrial complex) in the study region. The meteorological and atmospheric pollution data, the object of this study, are collected hourly from January to December 2019, the period with the most complete data available. The Malembá station is located in a public square in the municipality of Candeias, a rural region with many houses. The Malembá station is a little further from the port than the others, but it is more influenced by mobile sources as it is a more urbanized region. The Gamboa station is located in an Atlantic forest region, a rural and sparsely inhabited area, positioned on high ground, 600 m away from the sea coast. The Botelho station is located on the beach of Botelho (in the island of Maré). The Botelho station is located on the sea line, 2 km by sea from the port of Aratu. The port of Aratu has a large flow of trucks due to its cargo handling.

2.2. Experimental Data

The monitoring of air quality and the meteorological variables studied aims to meet what is established in the Technical Cooperation Term (TCT) signed between the State Public Ministry (SPM), the Institute of Environment and Water Resources of Bahia (INEMA), the Brazilian Institute of Environment and Renewable Natural Resources (IBAMA), the

Camaçari Industrial Development Committee (COFIC), the Bahia State Docks Company (CODEBA) and the Environmental Protection Company (CETREL). The TCT is made up of public and private organizations. The purpose of its implementation was to meet a legal obligation imposed by the SPM, repairing environmental damage caused by the factories to the local community, according to [39,40]. However, even though the monitoring network is of great importance to the health of the local community, its operation was suspended in February 2020 due to the termination of the legal obligation that created the TCT and the costs of operating the stations.

The air quality of the port complex is continuously monitored by monitoring stations located in Botelho, Gamboa and Malembá [41], as shown in Figure 1. The pollutants evaluated in this study are NOx (nitrogen oxide), O_3 (ozone) and PM10 (particulate matter smaller than 10 μm). Observations of meteorological variables and pollutant concentrations are reported as hourly average values for the year 2019. In this sense, a preliminary analysis of the behavior of meteorological variables (humidity, solar irradiation, temperature and wind speed) during the period under analysis is important. Figure 2 shows the behavior of the monthly average of each meteorological variable.

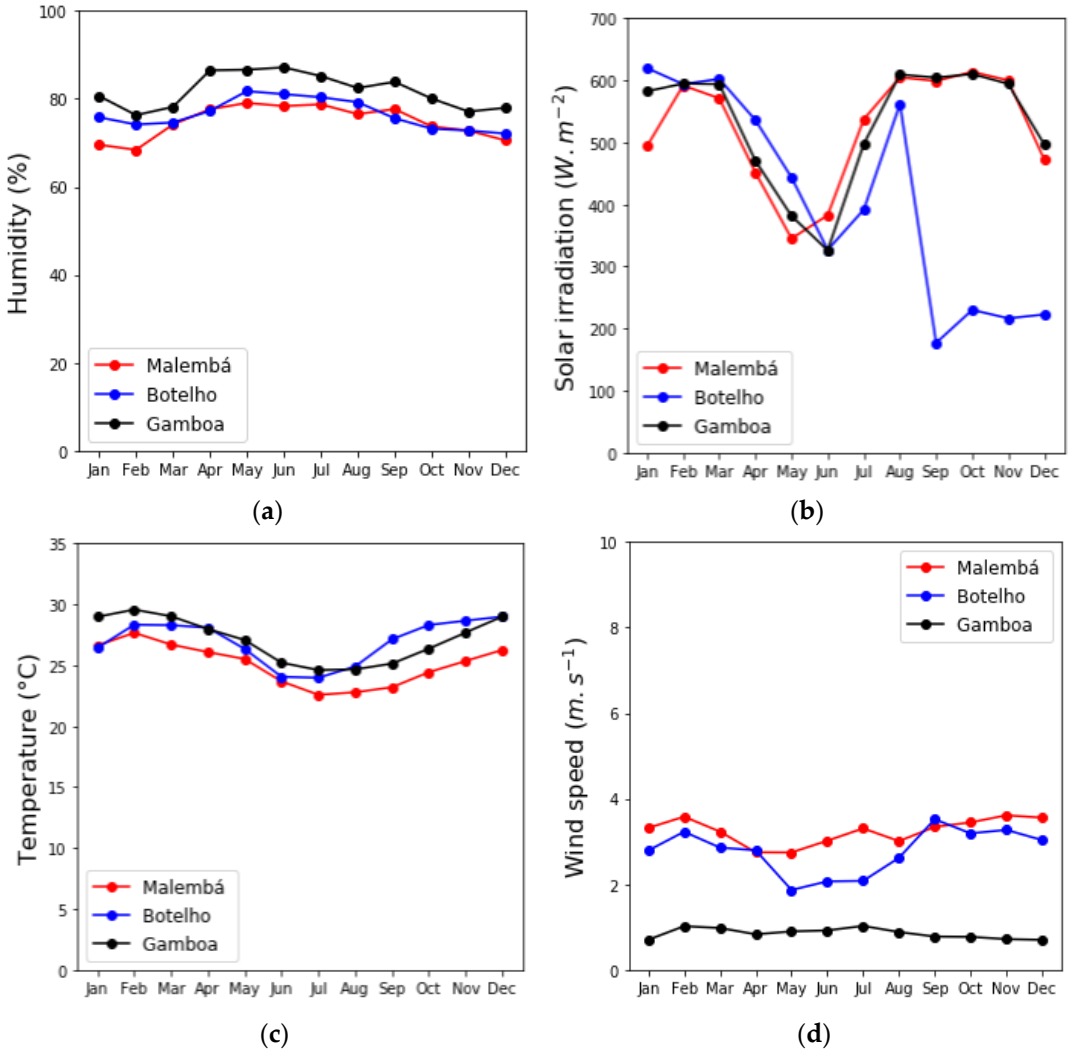

Figure 2. Meteorological variables: (**a**) humidity, (**b**) solar radiation, (**c**) temperature and (**d**) wind speed.

Figure 2 shows how the meteorological variables portray the characteristics of the location of each station. Gamboa, for example, has higher humidity and lower wind speed than the other two for all months of the year. When evaluating solar irradiation, Botelho has higher values during the summer (January–May), and for the other months, its solar

irradiation profile is lower. A sudden drop in solar irradiation is observed at the Botelho station (Figure 2b) in the months of September–October–November–December, which must have occurred due to the presence of more constant clouds in the region (station located on an island). Malembá and Botelho have similar behaviors for wind speed. However, Malembá has more constant winds on average. Regarding the wind direction, Figure 3 shows that the wind increased during the study period.

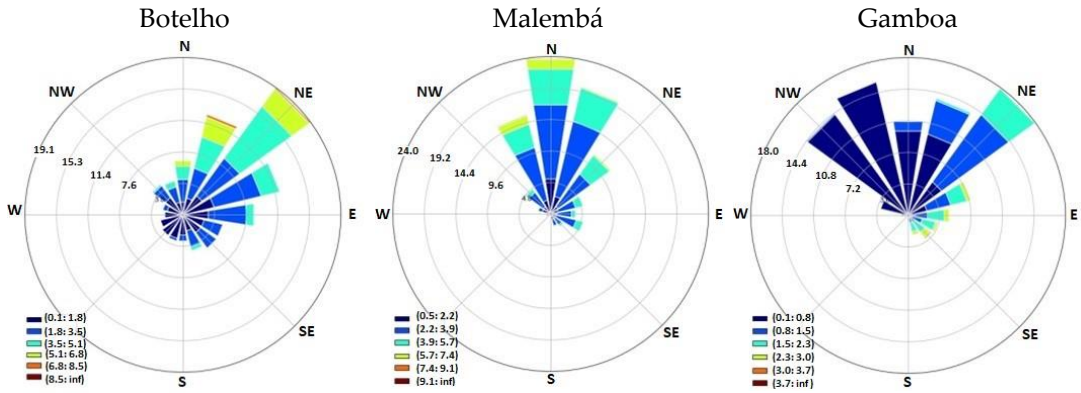

Figure 3. Wind increased for all stations.

Figure 3 shows a higher intensity preferential wind (3.5 to 6 ms^{-1}) coming from the NE to the Botelho station. For the Malembá station, higher intensity winds (3.9 to 7 ms^{-1}) are observed coming from the N direction. For the Gamboa station, wind is also observed coming from the NE/E direction (1.5 to 3 ms^{-1}). However, at this station, most of the time, the NW wind has low intensity (0.1 to 0.8 ms^{-1}). This is due, in part, to the presence of many trees (forest) in its surroundings.

Figure 4 shows the behavior of concentrations with monthly averages at the three monitoring stations.

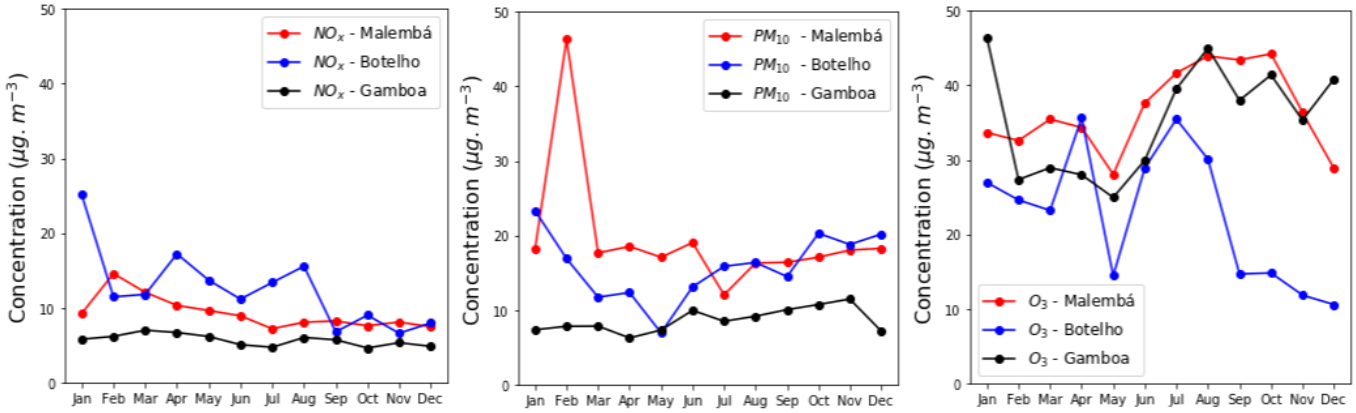

Figure 4. Monthly average for the concentration of pollutants: (**a**) NOx, (**b**) PM10 and (**c**) O_3.

When analyzing Figure 4, we observed that the highest levels of NOx were collected by the Botelho station, which is closer to the port of Aratu and petrochemical industries. The Malembá station had the second highest concentration and also is located close to petrochemical industries. In addition, both stations had higher wind speeds (Figure 2d), a factor that may contribute to the collection of higher concentrations of NOx from other regions. The Malembá and Gamboa stations show the highest concentrations of O_3, but due to their locations, these concentrations probably originated from distant emitting sources, driven by the preferential wind. It is important to highlight that the Botelho station had a drop in the average O_3 in the months that coincided with the drop in solar irradiation.

Botelho and Malembá indicated the highest concentrations of PM10 (peak in Malembá in February), where the values are justified by the characteristics of the geographical positions of these stations. Botelho is located near a port area with heavy vehicle movement, in addition to industries. In this sense, Malembá is located close to petrochemical industries and has a region with a greater flow of vehicles.

Taking into account the hourly data of global solar irradiation, air temperature, relative humidity and wind speed (meteorological variables) and O_3, NOx and PM10 (pollutants), we studied the relationship between pollutant concentrations and four different climatic variables.

2.3. DFA, DCCA and ρ_{DCCA}

In this paper, we use two different methodologies, the Detrended Fluctuation Analysis (DFA) and the Detrended Cross-Correlation Analysis Correlation Coefficient (ρ_{DCCA}), to analyze the behavior of different time series. By estimating the DFA, which was applied for the evolution of the pollutant concentrations, we want to assess the long-range dependence of those concentrations. With the ρ_{DCCA}, which we performed to analyze the long-range cross-correlation between the concentrations and four different climate variables, we want to assess the correlation between variables.

The DFA, applied to individual time series, is calculated with the following procedures. Based on a given time series x_t of length N, the first step calculates the profile $X_t = \sum_{i=1}^{t}(x_i - \langle x \rangle)$, with $\langle x \rangle$ as the mean observed value of the original time series. That profile is then divided into different time windows of length n, and for each window, using the ordinary least squares, the local trend $\widetilde{X}_t$ is calculated and used to detrend the profile X_t, i.e.,

$$F(n) = \sqrt{\frac{1}{N}\sum_{t=1}^{N}\left(X_t - \widetilde{X}_t\right)^2}.$$

This same process is repeated considering the different window sizes of dimension n. The DFA ends calculating the log-log regression between x and n, resulting in a power-law given by $F(n) \propto n^{\alpha}$, with α being equivalent to the Hurst exponent, and interpreted as follows: if a random walk describes the time series, if $0.5 < \alpha < 1$, the time series has a persistent behavior; if $\alpha < 0.5$, the time series has an anti-persistent behaviour. As we wanted to evaluate the evolution of the Hurst exponent over time, we applied a sliding windows approach, with windows of 500 observations, which allowed us to obtain sequenced Hurst exponents.

Proposed by [15], the DFA has been used in several research areas, including climatology and the emission of gases [21–23,42–45]. While the DFA analyzes the long-range dependence in individual time series, the DCCA analyzes cross-correlation dependence between pairs of time series, and the rationale of the methodology is similar to the DFA. In this case, the DCCA considers different time series x_t and y_t, with the same time length, and starts with the calculation of the profiles and $Y_t = \sum_{i=1}^{t}(y_i - \langle y \rangle)$, representing $\langle . \rangle$, the mean observed value of the respective variable. After dividing the profiles into different boxes of length n, the local trends are also calculated based on the ordinary least squares and from the detrended series. The covariance of the residuals is calculated and given by

$$f^2_{DCCA}(n) = \frac{1}{n-1}\sum_{k=i}^{i+n}\left(X_k - \widetilde{X}_k\right)\left(Y_k - \widetilde{Y}_k\right)$$

being the base of the calculation of the detrended covariance provided by

$$F^2_{DCCA}(n) = \frac{1}{N-n}\sum_{i=1}^{N-n} f^2_{DCCA}.$$

This DCCA was proposed by [35]. Combining both the DFA and DCCA, [24] proposes the DCCA correlation coefficient given by $\rho_{DCCA} = \frac{F^2_{DCCA}}{F_{DFA\{x\}}F_{DFA\{y\}}}$. This correlation coefficient, which we apply to analyze the cross-correlation between the emission of gases

and some climate variables, is efficient [25,34] and is testable according to the procedure of [46], which we used to obtain the confidence levels to perform that test. DCCA and its developments were already used in climatology and the study of the emission of gases by NOx, O_3 and PM10.

3. Results

We started our analysis by calculating the DFA exponents for the concentration of the pollutants at the three stations [47,48]. As we aimed to analyze the evolution over time, a sliding windows approach was used, with the results depicted in Figure 5 for Botelho, Gamboa and Malembá stations.

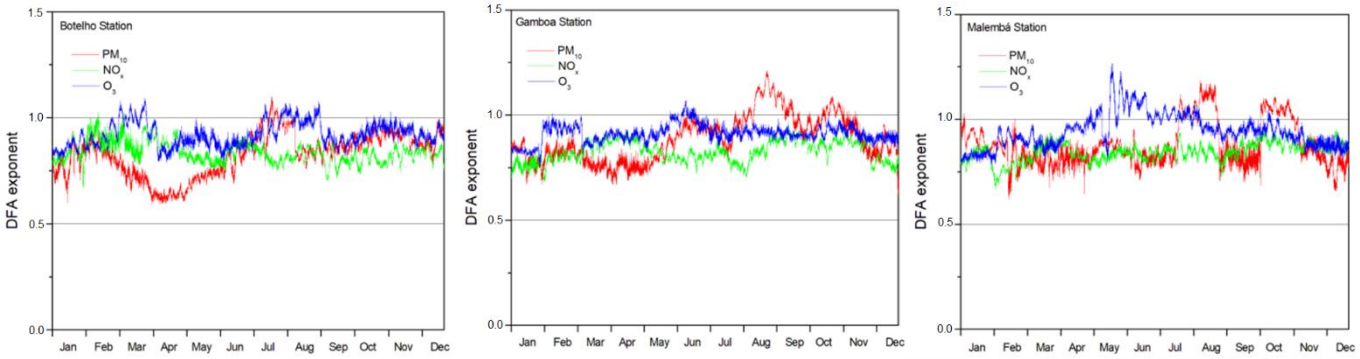

(**a**) (**b**) (**c**)

Figure 5. Evolution of the DFA exponents, considering a sliding window of 500 observations, for the pollutant concentrations (PM10, NOx, O_3): (**a**) Botelho; (**b**) Gamboa; (**c**) Malembá.

There, it is possible to identify that in all cases, the concentrations are described by Hurst exponents above 0.5, meaning that the concentrations do not follow random patterns. In most cases, the Hurst exponent is between 0.5 and 1, which means that the concentrations have a persistent behavior; other higher levels more likely follow, i.e., higher levels of concentrations. In some cases, it is possible to identify that some concentrations have a Hurst exponent above 1. This happens, for example, at the Botelho station during part of the year 2019 for O_3 and PM10, although to a lesser extent. This also happens at the Gamboa station with PM10, but for a smaller time extension, while at the Malembá station, the evidence is lower, although also happening with O_3 and PM10. A Hurst exponent higher than 1 implies that during those sliding windows, the series is non-stationary, which could be understood as uncontrolled concentration [49].

Figure 6 shows the ρ_{DCCA} between wind speed and concentrations at the different stations.

We identified a positive cross-correlation between O_3 and wind velocity, temperature and solar irradiation for smaller temporal scales (~24 h–1 day) at all stations, with more evidence at the Gamboa station. However, this correlation is more pronounced with the temperature variable. For the wind variable, at the Gamboa station, there is a decrease in the correlation up to 400 h, remaining constant until 800 h, decreasing smoothly, but remaining positive and small until the end of the period. For the Botelho station, there is also a decrease up to 400 h, but with a tendency to increase the correlation until the end of the period. At the Malembá station, there is a lower correlation, remaining similar until the end of the period. For the temperature variable, at all monitoring stations, there is a decrease in the correlation up to approximately 200 h. At the Malembá station, from 200 h onwards, a negative correlation begins, where for Botelho and Gamboa stations, it starts at 800 h. For the variable solar irradiation, at the Botelho station, it has a low positive correlation, reaching a peak up to 100 h and becoming negative after 200 h. For the Gamboa station, a small peak of positive correlation appears around 24 h, but quickly becomes negative, returning to increasing positive around 1100 h. The Malembá station already starts with a negative correlation, becoming positive and increasing around 200 h. For

the humidity variable, O_3 is strongly anti-correlated for all stations within a day. At the Malembá station, it reaches a positive correlation around 300 h, remaining positive, but small, until the end of the period.

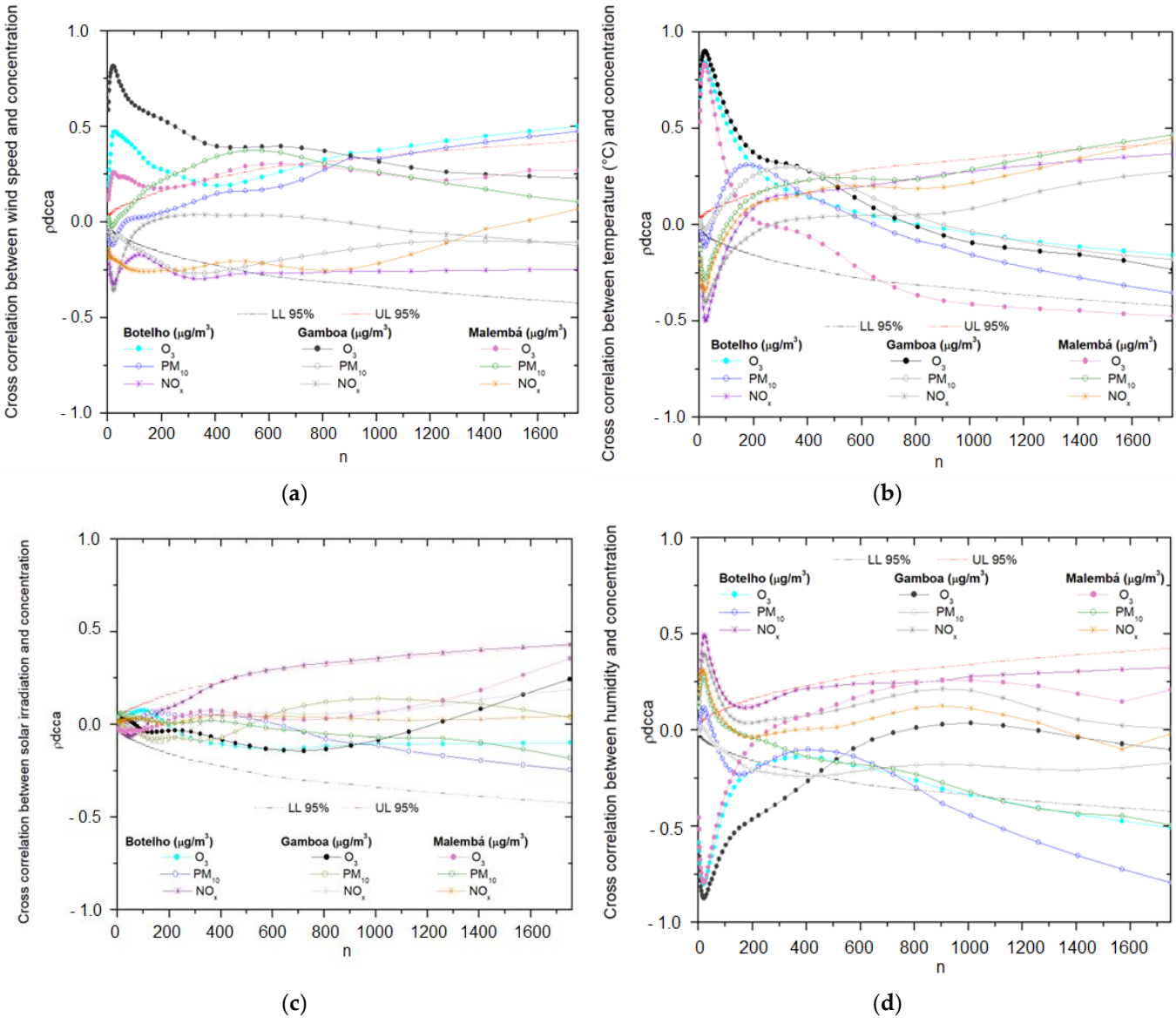

Figure 6. *ρDCCA* between (**a**) wind speed, (**b**) temperature, (**c**) solar irradiation, (**d**) humidity and concentrations in the different stations. Dashed lines refer to the critical levels to analyze the statistical significance of the correlations, considering a 95% confidence level.

Regarding PM10, we identified a negative cross-correlation between wind velocity, temperature and solar irradiation for smaller temporal scales (1 day) at all stations. For the wind variable at the Botelho station, around 100 h, the correlation becomes positive until the end of the period. For the Malembá station, the correlation becomes positive at 50 h, reaching a maximum around 500 h, then decreases, but remains positive. At the Gamboa station, it remains negative until the end of the period. For the temperature variable, the three stations present a negative correlation, with a maximum around 24 h. For the Botelho station, it starts to be positive around 50 h, reaching a maximum at 200 h, becoming negative around 800 h until the end of the period. At the Gamboa station, it starts to be positive around 100 h and reaches a maximum at 400 h, becoming negative at 1000 h. At the Malembá station, it becomes positive around 150 h with a tendency to increase until the end of the period. For

the variable solar irradiation, negligible behavior is observed. For the humidity variable, a greater positive correlation is observed for the Malembá station, becoming negative around 200 h and remaining until the end of the period. At the Botelho station, there is a positive correlation with a maximum in 24 h, becoming negative around 100 h. At the Gamboa station, there is a small negative correlation for almost the entire period.

In addition to this, we identified a negative cross-correlation between NOx and wind velocity for all temporal scales at all stations. For the temperature variable, the three stations present a negative correlation with a maximum around 24 h. For the Botelho station, it starts to be positive around 200 h, reaching a maximum at 200 h, with a smooth increase until the end of the period. At the Gamboa station, it starts to be positive around 400 h, remaining until the end of the period. At the Malembá station, it becomes positive around 200 h with a slight growth trend until the end of the period. At the Botelho station, for the variable solar irradiation, a positive growth is observed around 100 h until the end of the period. For Gamboa and Malembá stations, there are few variations. For the humidity variable, there is a positive correlation with a maximum around 24 h, decreasing up to 200 h for the three stations, but remaining small until the end of the period.

After this analysis, it is important to note that the state of Bahia is located in the tropics, and the tropical climate can change rapidly with convection and sea breeze and the weather is dominated by local, mesoscale and macroscale (synoptic) effects [44]. The winds in the tropics are usually light and variable, and in the coastal strip, the temperature and humidity are higher. Furthermore, it is important to mention that the winds are generated by the non-uniform heating of the Earth's surface. In addition, the topographic characteristics of a region also influence the behavior of the winds since, in a given area, differences in speed may lead to a reduction in wind speed. In this sense, it is well known that the local wind field is the result of a nonlinear interaction between the large-scale (synoptic) effects and local circulation. Because of this, the time series of wind speed is expected to be dependent on global and local circulations [44]. Fundamentally, the planetary boundary layer (PBL) is characterized by a diurnal cycle, indicating that the correlation and anti-correlation peaks in the meteorological variables studied here respond to forcings within a 24-h cycle, represented in Figure 6. The cycle is forced by solar irradiation, which heats the Earth's surface during the day, and the infrared radiation released into space cools the Earth's surface at night. These processes are influenced by external mesoscale forces, and the turbulence generated in the PBL arises from this interaction. The influence of larger time scales (mesoscale—week (~200 h); macroscale—month (~700 h)) is also noticed, related to variations in the correlations between meteorological variables and the concentration of each pollutant, in addition to the persistent and non-stationary character.

4. Conclusions

The results of this work contributed to advancing knowledge of different statistical methods. After the exploratory analyses, it was possible to identify a persistent influence of meteorological variables on the pollution process considering the entire period analyzed. The various studies analyzed and implemented show that data analysis guides control actions over time. In this sense, the concentrations of O_3, NOx and PM10 were mostly persistent, but with some periods where the system dynamics are characterized as non-stationary (transient regime or transient conditions). It is important to mention that NOx always had a persistent behavior at all monitoring stations. In addition, there was a greater correlation between concentration of O_3 and wind and also temperature in the three analyzed monitoring stations. Thus, with correlation between 0.5 and 1.0 for wind speed and O_3, the Gamboa station was up to 250 h (~10 days). In the same correlation interval, the temperature variable was up to 150 h (~6 days) (Gamboa), 100 h (~4 days) (Botelho) and 80 h (~3 days) (Malembá). It is important to highlight the strong negative correlation between humidity and O_3 concentration for all monitoring stations.

Using the DFA method, it was possible to identify in all cases that the concentrations are described by Hurst exponents above 0.5, meaning that the concentrations do not follow

random patterns. In most cases, the Hurst exponent is between 0.5 and 1, which means that the concentrations have a persistent behavior; other higher levels more likely follow, i.e., higher levels of concentrations. In some cases, the Hurst exponent is higher than 1, which implies that during those sliding windows, the series is non-stationary, which could be understood as uncontrolled concentration. On the other hand, the $\rho DCCA$ method was able to perceive the correlation between the studied meteorological variables and the pollution process to a certain extent; the results show physical coherence for the studied climatic events.

Our results show evidence that a reduction in pollutant emissions in the region under study could be stimulated by the state's environmental agency, particularly in relation to NOx (precursor of O_3), persistent in all months of the year. This type of pollutant comes from vehicular emissions, particularly from heavy vehicles (trucks, cranes, tractors), and from industrial processes, in addition to emissions from maneuvered and berthed ships. In this sense, this work represents an important advancement, as this is the first time that a more thorough statistical analysis has been carried out in this port region. In this way, the results could serve as a basis for a larger study with the objective of outlining mitigating strategies and effective practices to reduce the impact of emissions from both maritime transport, as well as all associated port activities, promoting better management and protection of air quality in the region.

This paper presents an unprecedented approach, emphasizing the difficulty of accessing an air quality database, with its limitations related to the lack of access to a database for a longer period, and its analysis is restricted to the domains of the Port Authority. The continuous assessment of air quality is important for the local community; even with this importance, due to the cost of operation and the termination of the legal obligation that created the working group responsible for their operation, these stations stopped operating in February of 2020. Authorities face the need to balance concerns between known impacts on human health and the environment with improving or maintaining economic development; using science is key to that balance. As our knowledge has better application in the science of air pollution, we can better predict, assess and mitigate the implications of air pollution on economic systems. Finally, it is believed that the methodology adopted in this article can serve as another form of analysis of this type of event for private and governmental institutions and researchers interested in the topic. Future work should address the analysis of other monitoring stations deployed in different zones of the MRS, as well as the use of the state of the art in numerical models (meteorological and pollutant dispersion) to assess whether these models effectively capture the long-range processes perceived in the data measured in the study region.

Author Contributions: Conceptualization, A.P., É.P., P.F., L.M.D.-V. and D.M.M.; methodology, A.P., É.P., P.F., L.M.D.-V. and D.M.M.; formal analysis, A.P., É.P., P.F., L.M.D.-V. and D.M.M.; writing—original draft preparation, A.P., É.P., P.F., L.M.D.-V. and D.M.M.; writing—review and editing, A.P., É.P., P.F., L.M.D.-V. and D.M.M. All authors have read and agreed to the published version of the manuscript.

Funding: Paulo Ferreira is pleased to acknowledge financial support from Fundação para a Ciência e a Tecnologia (grant UIDB/05064/2020).

Institutional Review Board Statement: Not applicable.

Informed Consent Statement: Not applicable.

Data Availability Statement: The data presented in this study are available on request from the corresponding author.

Conflicts of Interest: The authors declare no conflict of interest.

References

1. Yuan, X.; Zhang, M.; Wang, Q.; Wang, Y.; Zuo, J. Evolution analysis of environmental standards: Effectiveness on air pollutant emissions reduction. *J. Clean. Prod.* **2017**, *149*, 511–520. [CrossRef]
2. Cuhadaroglu, B.; Demirci, E. Influence of some meteorological factors on air pollution in Trabzon city. *Energy Build.* **1997**, *25*, 179–184. [CrossRef]
3. Tai, A.P.; Mickley, L.J.; Jacob, D.J. Correlations between fine particulate matter (PM2.5) and meteorological variables in the United States: Implications for the sensitivity of PM2.5 to climate change. *Atmos. Environ.* **2010**, *44*, 3976–3984. [CrossRef]
4. Meraz, M.; Rodriguez, E.; Femat, R.; Echeverria, J.C.; Alvarez-Ramirez, J. Statistical persistence of air pollutants (O_3, SO2, NO2 and PM10) in Mexico City. *Phys. A Stat. Mech. Appl.* **2015**, *427*, 202–217. [CrossRef]
5. Zhang, C.; Ni, Z.; Ni, L. Multifractal detrended cross-correlation analysis between PM2.5 and meteorological factors. *Phys. A Stat. Mech. Appl.* **2015**, *438*, 114–123. [CrossRef]
6. Todorov, V.; Dimov, I. Innovative Digital Stochastic Methods for Multidimensional Sensitivity Analysis in Air Pollution Modelling. *Mathematics* **2022**, *10*, 2146. [CrossRef]
7. Dimov, I.; Todorov, V.; Sabelfeld, K. A study of highly efficient stochastic sequences for multidimensional sensitivity analysis. *Monte Carlo Methods Appl.* **2022**, *28*, 1–12. [CrossRef]
8. Penenko, A.; Penenko, V.; Tsvetova, E.; Gochakov, A.; Pyanova, E.; Konopleva, V. Sensitivity Operator Framework for Analyzing Heterogeneous Air Quality Monitoring Systems. *Atmosphere* **2021**, *12*, 1697. [CrossRef]
9. Lin, H.; Wang, M.; Duan, Y.; Fu, Q.; Ji, W.; Cui, H.; Jin, D.; Lin, Y.; Hu, K. O_3 Sensitivity and Contributions of Different NMHC Sources in O_3 Formation at Urban and Suburban Sites in Shanghai. *Atmosphere* **2020**, *11*, 295. [CrossRef]
10. Zohdirad, H.; Namin, M.; Ashrafi, K.; Aksoyoglu, S.; Prévôt, A. Temporal variations, regional contribution, and cluster analyses of ozone and NOx in a middle eastern megacity during summertime over 2017–2019. *Environ. Sci. Pollut. Res.* **2022**, *29*, 16233–16249. [CrossRef]
11. Tsonis, A.A.; Roebber, P.J.; Elsner, J.B. Long-range correlations in the extratropical atmospheric circulation: Origins and implications. *J. Clim.* **1999**, *12*, 1534–1541. [CrossRef]
12. Glahn, B.; Gilbert, K.; Cosgrove, R.; Ruth, D.; Sheets, K. The gridding of MOS. *Weather Forecast.* **2009**, *24*, 520–529. [CrossRef]
13. Penereiro, J.C.; Ferreira, D.H.L. A Modelagem Matemática Aplicada às Questões Ambientais: Uma abordagem didática no estudo da precipitação pluviométrica e da vazão de rios. *Millenium* **2012**, *42*, 27–47.
14. Kurnaz, M.L. Application of detrended fluctuation analysis to monthly average of the maximum daily temperatures to resolve different climates. *Fractals* **2004**, *12*, 365–373. [CrossRef]
15. Peng, C.K.; Buldyrev, S.V.; Havlin, S.; Simons, M.; Stanley, H.E.; Goldberger, A.L. Mosaic organization of DNA nucleotides. *Phys. Rev. E* **1994**, *49*, 1685. [CrossRef]
16. Koscielny-Bunde, E.; Bunde, A.; Havlin, S.; Roman, H.E.; Goldreich, Y.; Schellnhuber, H.J. Indication of a universal persistence law governing atmospheric variability. *Phys. Rev. Lett.* **1998**, *81*, 729. [CrossRef]
17. Kavasseri, R.G.; Nagarajan, R. Evidence of crossover phenomena in wind-speed data. *IEEE Trans. Circuits Syst. I Regul. Pap.* **2004**, *51*, 2255–2262. [CrossRef]
18. Koçak, K. Examination of persistence properties of wind speed records using detrended fluctuation analysis. *Energy* **2009**, *34*, 1980–1985. [CrossRef]
19. De Oliveira Santos, M.; Stosic, T.; Stosic, B.D. Long-term correlations in hourly wind speed records in Pernambuco, Brazil. *Phys. A Stat. Mech. Appl.* **2012**, *391*, 1546–1552. [CrossRef]
20. Dos Anjos, P.S.; da Silva, A.S.A.; Stošić, B.; Stošić, T. Long-term correlations and cross-correlations in wind speed and solar radiation temporal series from Fernando de Noronha Island, Brazil. *Phys. A Stat. Mech. Appl.* **2015**, *424*, 90–96. [CrossRef]
21. Matsoukas, C.; Islam, S.; Rodriguez-Iturbe, I. Detrended fluctuation analysis of rainfall and streamflow time series. *J. Geophys. Res.: Atmos.* **2000**, *105*, 29165–29172. [CrossRef]
22. Chen, X.; Lin, G.; Fu, Z. Long-range correlations in daily relative humidity fluctuations: A new index to characterize the climate regions over China. *Geophy. Res. Lett.* **2007**, *34*, L07804. [CrossRef]
23. Caldeira, R.; Fernández, I.; Pacheco, J.M. On NAO's predictability through the DFA method. *Meteorol. Atmos. Phys.* **2007**, *96*, 221–227. [CrossRef]
24. Zebende, G.F. DCCA cross-correlation coefficient: Quantifying level of cross-correlation. *Phys. A Stat. Mech. Appl.* **2011**, *390*, 614–618. [CrossRef]
25. Kristoufek, L. Measuring correlations between non-stationary series with DCCA coefficient. *Phys. A Stat. Mech. Appl.* **2014**, *402*, 291–298. [CrossRef]
26. Kwapień, J.; Oświęcimka, P.; Drożdż, S. Detrended fluctuation analysis made flexible to detect range of cross-correlated fluctuations. *Phys. Rev. E* **2015**, *92*, 052815. [CrossRef]
27. Zebende, G.F.; da Silva Filho, A.M. Detrended multiple cross-correlation coefficient. *Phys. A Stat. Mech. Appl.* **2018**, *510*, 91–97. [CrossRef]
28. Ferreira, P.; Pereira, É.J.D.A.L.; da Silva, M.F.; Pereira, H.B. Detrended correlation coefficients between oil and stock markets: The effect of the 2008 crisis. *Phys. A Stat. Mech. Appl.* **2019**, *517*, 86–96. [CrossRef]
29. Ferreira, P.; Pereira, É. Contagion effect in cryptocurrency market. *J. Risk Financ. Manag.* **2019**, *12*, 115. [CrossRef]

30. Brito, A.D.A.; Araújo, H.A.D.; Zebende, G.F. Detrended multiple cross-correlation coefficient applied to solar radiation, air temperature and relative humidity. *Sci. Rep.* **2019**, *9*, 1–10.
31. Marinho, E.B.S.; Sousa, A.M.Y.R.; Andrade, R.F.S. Using detrended cross-correlation analysis in geophysical data. *Phys. A Stat. Mech. Appl.* **2013**, *392*, 2195–2201. [CrossRef]
32. Wang, G.J.; Xie, C.; Chen, S.; Han, F. Cross-correlations between energy and emissions markets: New evidence from fractal and multifractal analysis. *Math. Probl. Eng.* **2014**, *2014*, 197069. [CrossRef]
33. Zebende, G.F.; da Silva, M.F.; Machado Filho, A. DCCA cross-correlation coefficient differentiation: Theoretical and practical approaches. *Phys. A Stat. Mech. Appl.* **2013**, *392*, 1756–1761. [CrossRef]
34. Zhao, X.; Shang, P.; Huang, J. Several fundamental properties of DCCA cross-correlation coefficient. *Fractals* **2017**, *25*, 1750017. [CrossRef]
35. Podobnik, B.; Stanley, H.E. Detrended cross-correlation analysis: A new method for analyzing two nonstationary time series. *Phys. Rev. Lett.* **2008**, *100*, 084102. [CrossRef]
36. Vassoler, R.T.; Zebende, G.F. DCCA cross-correlation coefficient apply in time series of air temperature and air relative humidity. *Phys. A Stat. Mech. Appl.* **2012**, *391*, 2438–2443. [CrossRef]
37. Zebende, G.F.; Brito, A.A.; Silva Filho, A.M.; Castro, A.P. ρDCCA applied between air temperature and relative humidity: An hour/hour view. *Phys. A Stat. Mech. Appl.* **2018**, *494*, 17–26. [CrossRef]
38. Silva, A.B. Análise em Componentes Principais das Condições Atmosféricas em Episódios de Rajadas de Vento na Região Metropolitana de Salvador. Master's Thesis, Universidade Federal de Campinas, Campinas, Brazil, 2014.
39. CETREL. Monitoramento da Biodisponibilidade dos Poluentes no Meio Aquático do Entorno da Ilha de Maré. 2012. Available online: http://www.ceama.mpba.mp.br/boletim-informativo/doc_view/1999-relatorio-finalmonitoramento-ilha-de-mare.html (accessed on 13 September 2022).
40. Sousa, P.K.D. O Papel da Oceanografia na Gestão Portuária: Caso do Porto de Aratu e sua Relação com as Comunidades de Ilha de Maré. Bachelor Thesis, Universidade Federal da Bahia, Salvador, Brazil, 2017.
41. Companhia das Docas do Estado da Bahia (CODEBA). Características Ambientais da Área de Influência dos Portos. Available online: http://www.codeba.com.br/eficiente/sites/portalcodeba/pt-br/site.php?secao=apresentacao&sm=menu_esquerdo_meio_ambiente (accessed on 13 September 2022).
42. Siwy, Z.; Ausloos, M.; Ivanova, K. Correlation studies of open and closed state fluctuations in an ion channel: Analysis of ion current through a large-conductance locust potassium channel. *Phys. Rev. E* **2002**, *65*, 031907. [CrossRef]
43. Orun, M.; Koçak, K. Application of detrended fluctuation analysis to temperature data from Turkey. *Int. J. Climatol.* **2009**, *29*, 2130–2136. [CrossRef]
44. Santos, J.V.C.; Moreira, D.M.; Moret, M.A.; Nascimento, E.G.S. Analysis of long-range correlations of wind speed in different regions of Bahia and the Abrolhos Archipelago, Brazil. *Energy* **2019**, *167*, 680–687. [CrossRef]
45. Santos, J.V.C.; Perini, N.B.; Moret, M.A.; Nascimento, E.G.S.; Moreira, D.M. Scaling behavior of wind speed in the coast of Brazil and the South Atlantic Ocean: The crossover phenomenon. *Energy* **2021**, *217*, 119413. [CrossRef]
46. Podobnik, B.; Jiang, Z.Q.; Zhou, W.X.; Stanley, H.E. Statistical tests for power-law cross-correlated processes. *Phys. Rev. E* **2011**, *84*, 066118. [CrossRef] [PubMed]
47. Shen, C. A comparison of principal components using TPCA and nonstationary principal component analysis on daily air-pollutant concentration series. *Phys. A Stat. Mech. Appl.* **2017**, *467*, 453–464. [CrossRef]
48. Shen, C.H.; Li, C.L.; Si, Y.L. A detrended cross-correlation analysis of meteorological and API data in Nanjing, China. *Phys. A Stat. Mech. Appl.* **2015**, *419*, 417–428. [CrossRef]
49. Wang, G.J.; Xie, C. Cross-correlations between the CSI 300 spot and futures markets. *Nonlinear Dyn.* **2013**, *73*, 1687–1696. [CrossRef]